



Synthesis, Crystal Structure, Hirshfeld Surface, Energy Framework and Molecular Docking Analysis of Two Novel Carbazole Derivatives

G. DHANALAKSHMI¹, VELU SARAVANAN², ARASAMBATTU K. MOHANAKRISHNAN² and S. ARAVINDHAN^{1*}

¹Department of Physics, Presidency College (Autonomous), University of Madras, Chennai-600005, India

²Department of Organic Chemistry, University of Madras, Guindy Campus, Chennai-600025, India

*Corresponding author: E-mail: aravindhanpresidency@gmail.com

Received: 4 September 2019;

Accepted: 30 September 2019;

Published online: 16 November 2019;

AJC-19657

Carbazole derivatives are important compounds from medicinal point of view because of their widespread biological significance. In the present work two compounds 7-(4-chlorophenyl)-5-methyl-12-(phenylsulfonyl)-12H-naphtho[1,2-*b*]carbazole (**I**) and 7-ethyl-5-methyl-12-(phenylsulfonyl)-12H-naphtho[1,2-*b*]carbazole (**II**) have been synthesized and characterized by XRD, Hirshfeld surface, energy framework and docking analysis. Single crystal X-ray diffraction analysis shows that the compound **I** crystallizes in monoclinic system with space group P2₁/n whereas compound **II** crystallizes in triclinic with space group P-1. In both compounds there are two intramolecular C-H...O hydrogen bonds, which generates two S (6) ring motifs. The crystal packing is stabilized through weak C-H...O and C-H...Cl interactions. The molecules also features C-H... π interactions. The intermolecular interactions of both compounds were analyzed using Hirshfeld surface analysis and two dimensional fingerprint plots, which was confirmed by the XRD data. Energy frameworks were used to calculate the intermolecular interaction energies and their distribution over the crystal structure. Molecular docking studies show that the compounds exhibits antitumor activity.

Keywords: Carbazole, Intermolecular hydrogen bonds, Hirshfeld surface analysis, Energy framework, Molecular docking.

INTRODUCTION

Carbazole derivatives are heterocyclic compounds [1] which exhibit antitumour, antioxidative, anti-inflammatory [2] antifungal [3,4] antimutagenic [5-7], antimicrobial [8], anti-Alzheimer [9], pim kinase inhibitory [10] and cytotoxic activity properties [11]. Carbazole derivatives exhibit redox, luminescent properties and also has thermal and environmental stability. Carbazole derivatives are used in synthetic and medicinal chemists [12]. They are used in industrial applications of polyvinylcarbazole (PVCZ) in electrophotographic materials and in the production of organic light emitting diodes [13], colour displays, organic semiconductors, laser and solarcells [14]. Literature survey gives the idea that because of the wide band-gap energy, high triplet energy and hole-transporting competence [15,16] they are used as blue phosphorescent host materials. Carbazole derivatives are vital for the design of novel antitumor agents [17]. Now-a-days, different carbazole derivatives are used in photodynamic therapy [17-22]. They are also

used as precursor compounds for the synthesis of pyrido-carbazole alkaloids [23] and indole alkaloids [24]. It has been noticed that introduction of additional heterocyclic rings to the carbazole core tends to exert profound influence in increasing the anticancer activity.

Rechargeable batteries [25] and electrochromic displays [26] can be produced from carbazole based heterocyclic polymer systems and hence they are used as building blocks for the design and synthesis of molecular glasses, which are widely studied as components of electroactive and photoactive materials [27]. Carbazoles exhibit several pharmacological activities and are used in medicinal and synthetic organic chemists [28].

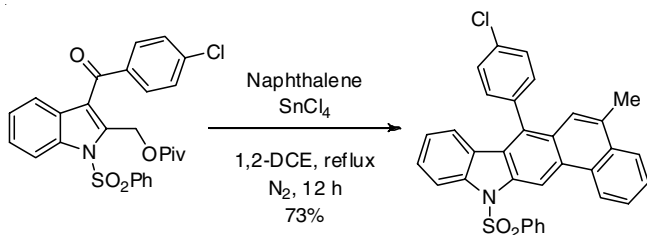
Among the aromatic hydrocarbon phenanthrene groups, carbazoles are very interesting heterocyclic derivatives. Since decades they are used in industrial applications of polyvinyl-carbazole (PVCZ) in electrophotographic materials [29]. Carbazole derivatives are precursors of materials used in electronics and photonics [30-33] which is used as an alternative for energy crisis. Remarkable studies have been done on 3,6-

substituted and 2,7-substituted carbazole derivatives [34-37]. Carbazole derivatives exhibits photoconductivity [38] and optical [39] properties. Carbazoles exhibits fluorescent properties, because of which they are used for the production of light emitting diodes (OLEDs) [40,41] and sensors [42-45]. For these reasons, there is a constant search for new carbazole derivatives as potential substrates for new materials with promising optoelectronic properties.

In this present work, the structures of compounds **I** and **II** and their intra- and intermolecular hydrogen bond interactions were determined by X-ray crystallography. The contribution percentage of intermolecular contacts in the crystal structure is determined with the fingerprint plots analyzed by the Hirshfeld surface technique. To analyze the nature of interactions present in the molecule, Hirshfeld surface and 2D fingerprint plot studies were performed. The intermolecular interaction energies were also calculated and their distribution over the crystal structure were visualized graphically using energy frameworks. Docking studies were performed using AUTODOCK software to check their binding interactions with selenium-containing target protein, thioredoxin reductase (PDB ID: 3QFA).

EXPERIMENTAL

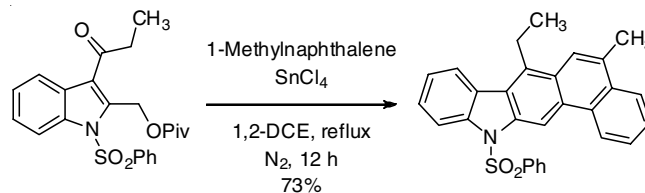
Synthesis of compound I: A solution of (3-(4-chlorobenzoyl)-1-(phenylsulfonyl)-1*H*-indol-2-yl)methyl pivalate (0.2 g, 0.39 mmol) in dry DCE (10 mL), SnCl₄ (0.122 g, 0.47 mmol) and 1-methylnaphthalene (0.061 g, 0.43 mmol) were added and refluxed for 12 h under nitrogen atmosphere. After the completion of the reaction, it was poured into ice water (30 mL) containing conc. HCl (3 mL). The organic layer was separated and the aqueous layer was extracted with DCM (2 × 20 mL). The combined organic layer was washed with water (2 × 20 mL) and over anhydrous Na₂SO₄. Removal of solvent followed by column chromatographic purification (silica gel, hexane:ethyl acetate 9:1) furnished 7-(4-chlorophenyl)-5-methyl-12-(phenylsulfonyl)-12*H*-naphtho[1,2-*b*]carbazole as a colourless solid (**Scheme-I**). Yield 0.152 g, 73 %; m.p. 228-230 °C. HRMS (EI, 70 eV): *m/z* calcd. for C₃₃H₂₂NO₂ClS [M⁺] 531.1060; Found 531.1057. Elemental analysis calcd. for C₃₃H₂₂NO₂ClS: C, 74.50; H, 4.17; N, 2.63; S, 6.03; Found C, 74.24; H, 4.03; N, 2.41; S, 6.26



Scheme-I: Synthetic route of compound **I**

Synthesis of compound II: A solution of (1-(phenylsulfonyl)-3-propionyl-1*H*-indol-2-yl)methyl pivalate (0.2 g, 0.47 mmol) in dry DCE (10 mL), SnCl₄ (0.146 g, 0.56 mmol) and 1-methylnaphthalene (0.073 g, 0.51 mmol) were added and refluxed for 12 h under nitrogen atmosphere. After the completion of the reaction, it was poured into ice water (30 mL) containing conc. HCl (3 mL). The organic layer was separated

and the aqueous layer was extracted with DCM (2 × 20 mL). The combined organic layer was washed with water (2 × 20 mL) and dried over Na₂SO₄. Removal of solvent followed by column chromatographic purification (silica gel, hexane:ethyl acetate 9:1) furnished 7-ethyl-5-methyl-12-(phenylsulfonyl)-12*H*-naphtho[1,2-*b*]carbazole as a colourless solid (**Scheme-II**). Yield 0.143 g, 68 %; m.p. 224-226 °C.



Scheme-II: Synthetic route of compound **II**

Characterization techniques: A Bruker AXS (Kappa Apex II) X-ray diffractometer was used for single crystal XRD studies at 296 K with graphite monochromatic MoK_α radiation of wavelength (λ) = 0.71073 Å. Hirshfeld surface analysis, energy framework and fingerprint plots were generated by Crystal Explorer (Version 17.5) program [46]. Molecular docking studies were performed using the software Autodock.

RESULTS AND DISCUSSION

X-ray crystallography: Data were corrected for Lorentz-polarization and absorption factors. The structure was solved by direct methods using SHELXT-2014/4 [47] and refined using SHELXL2014/7 [47], by full matrix least squares on F². All non-hydrogen atoms were refined anisotropically and H atoms were localized from the difference electron-density maps and refined as riding atoms with C-H = 0.93 or 0.97 Å with U_{iso}(H) = 1.5U_{eq}(C) for methyl H atoms and 1.2U_{eq}(C) for other H atoms. The geometrical calculations were carried out using the program PLATON [48]. The molecular and packing diagrams were generated using the software MERCURY [49].

The ORTEP diagrams of compounds **I** and **II** are shown in Fig. 1. The packing of the molecules of both compounds are shown in Fig. 2. The space group was deduced to be P2₁/n for compound **I** and P-1 for compound **II**, respectively. The structural overlap drawing shows that the overall conformation of two molecules is similar as shown in Fig. 3.

The geometric parameters of both the compounds agree well with those reported for closely related structures [50,51]. The carbazole skeleton in compound **I** and **II** are planar with maximum deviation of 0.0213(3) Å for atom C8 and 0.0310(9) Å for atom C13, respectively. The dihedral angle between the naphtho-carbazole ring (C8-C16) and the sulphonyl bound phenyl ring is 76.98(14)° in compound **I**, whereas in compound **II** it is 85.92(16)°.

In both compounds there are two intramolecular C-H...O hydrogen bonds, which generates two S(6) ring motifs. Atom S1 has a distorted tetrahedral geometry. The widening of the angle O1-S1-O2 [120.13(15)° Å in compound **I** and 119.99(1)° Å in compound **II**] and narrowing of angle N1---S1---C28 [105.26(14)° Å in compound **I** and N1---S1---C6 [104.89(14)° Å from the ideal tetrahedral value are attributed to the Thorpe-Ingold effect [52]. The widening of the angles

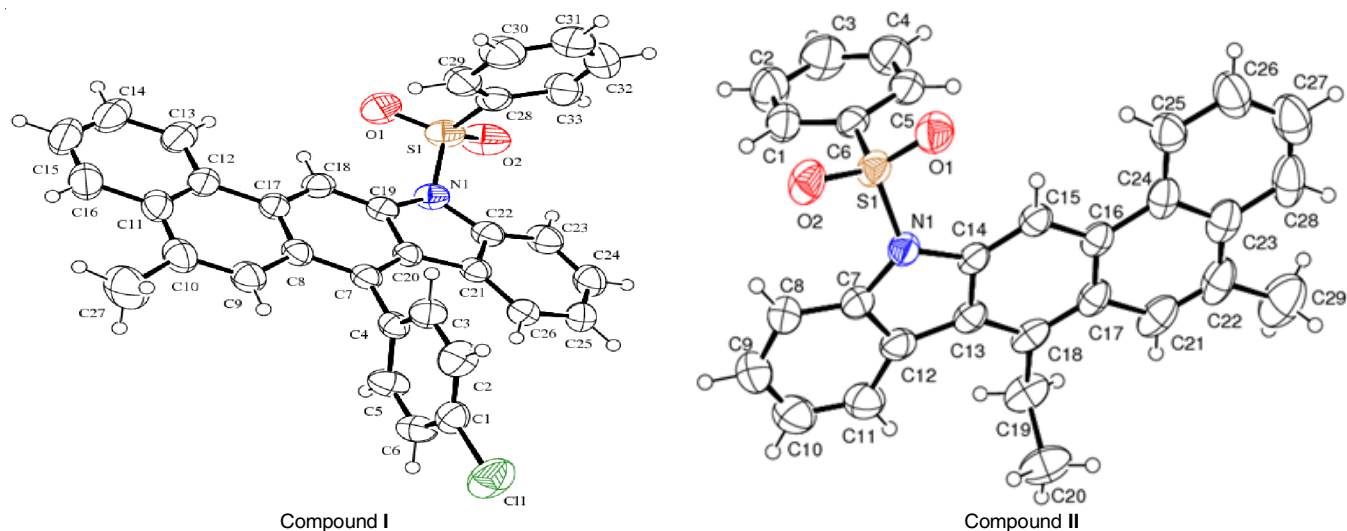


Fig. 1. Molecular structure of compounds **I** and **II** with 40 % probability displacement ellipsoids for non-H atoms

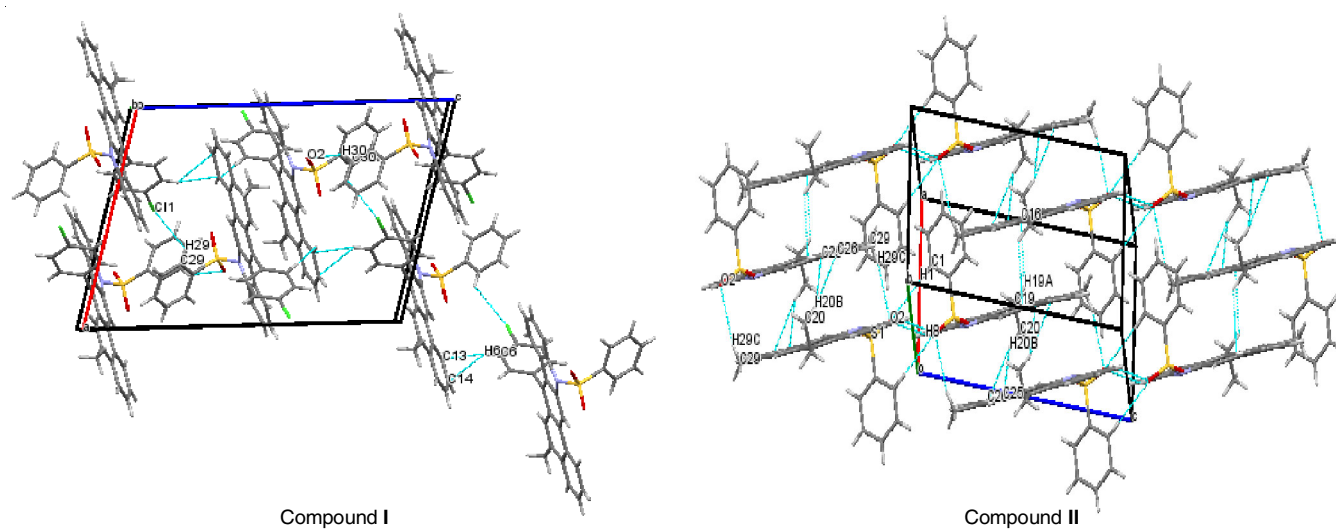


Fig. 2. Crystal packing of compounds **I** and **II** showing the intermolecular interactions

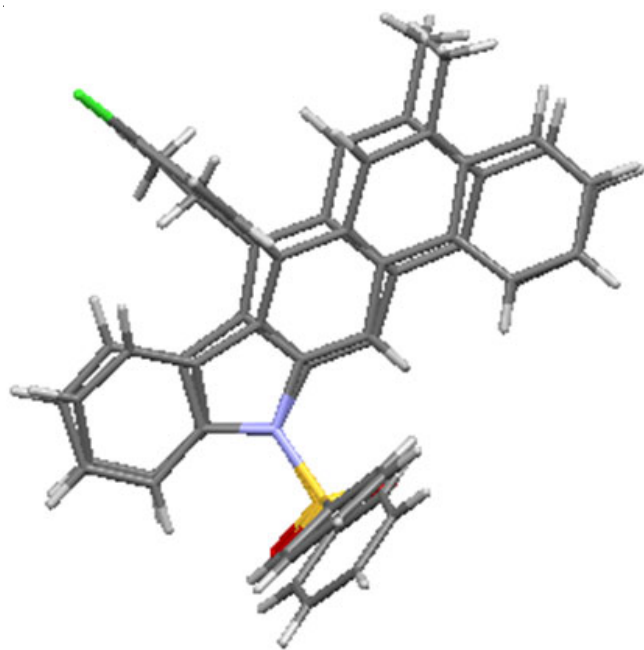


Fig 3. Structural overlap view of compounds **I** and **II**

may be due to the repulsive interaction between the two short S---O bonds. As a result of the electron-withdrawing character of the phenylsulfonyl group, the bond lengths [N1-C19 (1.432(3) Å) N1-C22 (1.429(4) Å)] in compound **I** and [N1-C7 (1.429(4) Å) and N1-C14 (1.433(4) Å)] in compound **II** are longer than the normal value of 1.355(14) Å [53]. In both compounds, sum of the bond angles around atom N1 are 347.92 (23)° and 351.21(2)°, indicating hybridization between sp^2 and sp^3 . The compounds are stabilized by intramolecular S (6) ring motifs with the sulfone oxygen atoms. The crystal data and structure refinement details are given in Table-1. The selected bond lengths, bond angles, torsion angles and hydrogen bonds are listed in Tables 2-5, respectively.

In compound **I** the molecules are linked by C30-H30...O2, C29-H29...C11, hydrogen bonds, whereas in compound **II** they are linked by C8-H8...O2, C23-H23...O2 interactions. Both compounds features C-H... π interactions, in compound **I** with C6-H6...Cg where Cg is the centroid of the six member ring [C11-C12-C13-C14-C15-C16] with C-Cg distance of 3.065 Å and H...Cg distance of 2.204 Å (symmetry code : -x, 1-y, 1-z) and in compound **II** with with C20-H20...Cg

TABLE-1
 CRYSTAL DATA AND STRUCTURE REFINEMENT FOR THE COMPOUNDS I AND II

	Compound I	Compound II
CCDC No	1569609	1867913
Empirical formula	C ₃₃ H ₂₂ NO ₂ ClS	C ₂₉ H ₂₃ NO ₂ S
Formula weight	532.02	449.54
Temperature	293(2) K	296(2) K
Wavelength	1.54178 Å	0.71073 Å
Crystal system	Monoclinic	Triclinic
Space group	P2 ₁ /n	P-1
Unit cell dimensions	a = 12.8572(3) Å; α = 90° b = 11.6802(4) Å; β = 105.198(6)° c = 17.9335(9) Å; γ = 90°	a = 8.2462(5) Å; α = 102.500(2)° b = 9.7832(6) Å; β = 93.222(2)° c = 14.2249(8) Å; γ = 92.127(2)°
Volume	2598.97(18) Å ³	1117.18(12) Å ³
Z	4	2
Density (calculated)	1.360 Mg/m ³	1.336 Mg/m ³
Absorption coefficient	2.304 mm ⁻¹	0.173 mm ⁻¹
F(000)	1104	472
Crystal size	0.100 mm × 0.100 mm × 0.050 mm	0.250 mm × 0.200 mm × 0.150 mm
Theta range for data collection	3.800 to 67.474°	3.233 to 24.997°
Index ranges	-14<=h<=15, -13<=k<=13, -21<=l<=20	-9<=h<=9, 11<=k<=13, 21<=l<=20
Reflections collected	28545	36661
Independent reflections	4627 [R(int) = 0.0500]	3902 [R(int) = 0.0499]
Completeness to θ = 67.474°	98.90 %	99.3 %
Absorption correction	Semi-empirical from equivalents	Semi-empirical from equivalents
Maximum and minimum transmission	0.7536 and 0.6117	0.7454 and 0.5014
Refinement method	Full-matrix least-squares on F ²	Full-matrix least-squares on F ²
Data/restraints/parameters	4627/0/343	3902/0/301
Goodness-of-fit on F ²	1.09	1.116
Final R indices [I>2σ(I)]	R1 = 0.0593, wR2 = 0.1431	R1 = 0.0633, wR2 = 0.1653
R indices (all data)	R1 = 0.0724, wR2 = 0.1525	R1 = 0.0829, wR2 = 0.1973
Largest diff. peak and hole	0.399 and -0.339 e. Å ⁻³	0.870 and -0.313 e. Å ⁻³

 TABLE-2
 SELECTED BOND LENGTHS (Å) OF COMPOUNDS I AND II

Compound I				Compound II			
Bond	Bond length (Å)						
C(1)-C(6)	1.367(5)	C(12)-C(13)	1.406(5)	C(1)-C(2)	1.381(5)	C(15)-C(16)	1.406(4)
C(1)-C(2)	1.376(5)	C(12)-C(17)	1.463(4)	C(1)-C(6)	1.385(5)	C(16)-C(17)	1.410(5)
C(2)-C(3)	1.367(5)	C(13)-C(14)	1.378(5)	C(2)-C(3)	1.376(6)	C(16)-C(24)	1.459(5)
C(3)-C(4)	1.388(4)	C(14)-C(15)	1.361(7)	C(3)-C(4)	1.385(7)	C(17)-C(18)	1.421(5)
C(5)-C(6)	1.369(4)	C(15)-C(16)	1.365(7)	C(4)-C(5)	1.376(6)	C(17)-C(21)	1.449(5)
C(7)-C(20)	1.385(4)	C(17)-C(18)	1.401(4)	C(5)-C(6)	1.386(4)	C(18)-C(19)	1.516(5)
C(7)-C(8)	1.424(4)	C(18)-C(19)	1.370(4)	C(7)-C(8)	1.382(5)	C(19)-C(20)	1.518(5)
C(8)-C(17)	1.414(4)	C(19)-C(20)	1.412(4)	C(7)-C(12)	1.401(5)	C(21)-C(22)	1.346(6)
C(8)-C(9)	1.436(4)	C(19)-N(1)	1.432(4)	C(7)-N(1)	1.429(4)	C(22)-C(23)	1.417(6)
C(9)-C(10)	1.353(5)	C(20)-C(21)	1.458(4)	C(8)-C(9)	1.380(6)	C(22)-C(29)	1.513(6)
C(10)-C(11)	1.440(5)	C(21)-C(26)	1.388(4)	C(9)-C(10)	1.381(7)	C(23)-C(24)	1.408(5)
C(11)-C(12)	1.402(5)	C(21)-C(22)	1.405(4)	C(10)-C(11)	1.366(6)	C(23)-C(28)	1.437(6)
C(11)-C(16)	1.434(5)	C(22)-C(23)	1.382(4)	C(11)-C(12)	1.396(5)	C(24)-C(25)	1.408(5)
				C(12)-C(13)	1.453(5)	C(25)-C(26)	1.363(5)
				C(13)-C(18)	1.402(4)	C(26)-C(27)	1.352(7)
				C(13)-C(14)	1.410(4)	C(27)-C(28)	1.368(7)
				C(14)-C(15)	1.365(4)	O(1)-S(1)	1.417(3)
				C(14)-N(1)	1.434(4)	O(2)-S(1)	1.422(2)

is the centroid of the six member ring [C23–C24–C25–C26–C27–C28]) with C–C_g distance of 3.793 Å and H...C_g distance of 3.676 Å (symmetry code: -x, -y+1, -z+1). Fig. 4 shows the crystal packing of compounds I and II featuring C–H...π interaction.

Hirshfeld surface analysis: The data obtained from single crystal XRD analysis were used to generate the Hirshfeld

surface [54,55]. Crystal Explorer version 17.5 software was used to analyze the intermolecular contacts by generating Hirshfeld surface using the CIF as input file. 2D fingerprint plots were used to see the graphical visualization of the intermolecular contacts. The factor d_{norm} has been used to analyze the intermolecular contacts with the combination of three colours red, blue and white. It comprises of two elements, d_e

TABLE-3
SELECTED BOND ANGLES (°) OF COMPOUNDS I AND II

Compound I				Compound II			
Bond	Bond angle (°)	Bond	Bond angle (°)	Bond	Bond angle (°)	Bond	Bond angle (°)
C(6)-C(1)-C(2)	121.0(3)	C(14)-C(15)-C(16)	119.6	C(2)-C(1)-C(6)	118.9(3)	C(5)-C(6)-S(1)	119.2(3)
C(3)-C(2)-C(1)	119.1(3)	C(14)-C(15)-H(15)	120.5(4)	C(2)-C(1)-H(1)	120.5	C(8)-C(7)-C(12)	122.7(3)
C(3)-C(2)-H(2)	120.4	C(15)-C(16)-H(16)	120.6(4)	C(6)-C(1)-H(1)	120.5	C(9)-C(8)-C(7)	117.1(4)
C(2)-C(3)-C(4)	121.6(3)	C(18)-C(17)-C(12)	119.9(2)	C(3)-C(2)-C(1)	119.9(4)	C(9)-C(8)-H(8)	121.4
C(5)-C(4)-C(3)	117.3(3)	C(8)-C(17)-C(12)	121.5(3)	C(3)-C(2)-H(2)	120.1	C(7)-C(8)-H(8)	121.4
C(5)-C(4)-C(7)	122.6(2)	C(18)-C(19)-C(20)	120.6	C(1)-C(2)-H(2)	120.1	C(8)-C(9)-C(10)	121.7(4)
C(3)-C(4)-C(7)	120.0(2)	C(23)-C(22)-C(21)	119.0(3)	C(2)-C(3)-C(4)	120.7(4)	C(8)-C(9)-H(9)	119.1
C(6)-C(5)-C(4)	122.0(3)	C(23)-C(22)-N(1)	121.3(3)	C(2)-C(3)-H(3)	119.6	C(10)-C(9)-H(9)	119.1
C(4)-C(5)-H(5)	119	C(24)-C(23)-H(23)	118.0(3)	C(4)-C(3)-H(3)	119.6	C(11)-C(10)-C(9)	120.4(4)
C(1)-C(6)-C(5)	118.9(3)	C(23)-C(24)-C(25)	121	C(5)-C(4)-C(3)	120.1(4)	C(11)-C(10)-H(10)	119.8
C(5)-C(6)-H(6)	120.5	C(23)-C(24)-H(24)	121.9(3)	C(5)-C(4)-H(4)	119.9	C(9)-C(10)-H(10)	119.8
C(7)-C(8)-C(9)	120.4(3)	C(26)-C(25)-C(24)	119.1	C(3)-C(4)-H(4)	119.9	C(10)-C(11)-C(12)	120.2(4)
C(10)-C(9)-C(8)	122.8(3)	C(26)-C(25)-H(25)	120.2(3)	C(4)-C(5)-C(6)	118.7(4)	C(10)-C(11)-H(11)	119.9
C(9)-C(10)-C(27)	119.2(4)	C(25)-C(26)-C(21)	119.9	C(4)-C(5)-H(5)	120.6	C(12)-C(11)-H(11)	119.9
C(11)-C(10)-C(27)	121.6(3)	C(29)-C(28)-C(33)	120.2	C(6)-C(5)-H(5)	120.6	C(11)-C(12)-C(7)	117.7(3)
C(12)-C(11)-C(10)	120.6(3)	C(33)-C(28)-S(1)	119.2(3)	C(1)-C(6)-C(5)	121.6(3)	C(18)-C(13)-C(14)	119.2(3)
C(11)-C(12)-C(13)	118.8(3)	C(30)-C(29)-C(28)	121.1(3)	C(1)-C(6)-S(1)	119.2(3)	C(14)-C(15)-H(15)	120.6
C(11)-C(12)-C(17)	119.7(3)	C(28)-C(29)-H(29)	119.5(3)				
C(13)-C(12)-C(17)	121.5(3)	C(31)-C(30)-H(30)	120.3				
C(14)-C(13)-C(12)	120.8(4)	C(32)-C(31)-C(30)	119.5				
C(15)-C(14)-C(13)	120.9(4)	C(30)-C(31)-H(31)	119.4(4)				
C(15)-C(14)-H(14)	119.6	C(31)-C(32)-H(32)	120.3				

TABLE-4
SELECTED TORSION ANGLES (Å) OF COMPOUNDS I AND II

Compound I				Compound II			
Bond	Torsion angle (°)						
Cl(1)-C(1)-C(2)-C(3)	179.8(2)	C(4)-C(7)-C(20)-C(19)	-177.0(2)	C(4)-C(5)-C(6)-S(1)	177.8(3)	C(21)-C(22)-C(23)-C(28)	-178.7(3)
C(2)-C(3)-C(4)-C(7)	-178.0(3)	C(8)-C(7)-C(20)-C(21)	-176.9(3)	N(1)-C(7)-C(8)-C(9)	-176.4(3)	C(22)-C(23)-C(24)-C(25)	-175.2(3)
C(7)-C(4)-C(5)-C(6)	177.8(3)	N(1)-C(19)-C(20)-C(7)	-178.1(2)	C(10)-C(11)-C(12)-C(13)	178.8(4)	C(28)-C(23)-C(24)-C(16)	-178.4(3)
Cl(1)-C(1)-C(6)-C(5)	-179.9(3)	C(18)-C(19)-C(20)-C(21)	177.3(2)	N(1)-C(7)-C(12)-C(11)	176.1(3)	C(17)-C(16)-C(24)-C(25)	173.5(3)
C(4)-C(7)-C(8)-C(17)	176.9(2)	C(19)-C(20)-C(21)-C(26)	-176.9(3)	C(8)-C(7)-C(12)-C(13)	-180.0(3)	C(15)-C(16)-C(24)-C(23)	175.9(3)
C(20)-C(7)-C(8)-C(9)	176.9(2)	C(7)-C(20)-C(21)-C(22)	178.1(3)	C(7)-C(12)-C(13)-C(18)	-179.4(3)	C(16)-C(24)-C(25)-C(26)	178.7(3)
C(7)-C(8)-C(9)-C(10)	-179.0(3)	C(20)-C(21)-C(22)-C(23)	-177.4(3)	C(11)-C(12)-C(13)-C(14)	-176.8(4)	C(22)-C(23)-C(28)-C(27)	178.0(4)
C(8)-C(9)-C(10)-C(27)	176.3(3)	C(26)-C(21)-C(22)-N(1)	177.2(2)	C(12)-C(13)-C(14)-C(15)	178.7(3)	C(8)-C(7)-N(1)-C(14)	-179.9(3)
C(27)-C(10)-C(11)-C(12)	-175.1(3)	N(1)-C(22)-C(23)-C(24)	-176.0(3)	C(18)-C(13)-C(14)-N(1)	-179.1(2)	C(15)-C(14)-N(1)-C(7)	-179.8(3)
C(9)-C(10)-C(11)-C(16)	-179.3(3)	C(20)-C(21)-C(26)-C(25)	176.5(3)	N(1)-C(14)-C(15)-C(16)	178.9(2)	C(7)-N(1)-S(1)-O(1)	172.9(2)
C(10)-C(11)-C(12)-C(13)	178.5(3)	S(1)-C(28)-C(29)-C(30)	179.8(3)	C(14)-C(15)-C(16)-C(24)	177.7(2)	C(21)-C(17)-C(18)-C(13)	177.4(3)
C(16)-C(11)-C(12)-C(17)	-179.5(3)	S(1)-C(28)-C(33)-C(32)	179.5(3)	C(24)-C(16)-C(17)-C(18)	-176.8(3)	C(16)-C(17)-C(18)-C(19)	175.5(3)
C(17)-C(12)-C(13)-C(14)	178.7(3)	C(23)-C(22)-N(1)-C(19)	177.2(3)	C(15)-C(16)-C(17)-C(21)	-177.2(3)	C(18)-C(17)-C(21)-C(22)	179.7(3)
C(10)-C(11)-C(16)-C(15)	-178.1(3)	C(18)-C(19)-N(1)-C(22)	-177.3(3)	C(12)-C(13)-C(18)-C(17)	-177.9(3)	C(17)-C(21)-C(22)-C(29)	180.0(4)
C(9)-C(8)-C(17)-C(18)	-176.8(2)	C(22)-N(1)-S(1)-O(1)	179.3(2)	C(14)-C(13)-C(18)-C(19)	-176.5(3)	C(29)-C(22)-C(23)-C(24)	178.8(3)
C(7)-C(8)-C(17)-C(12)	-179.7(2)	C(29)-C(28)-S(1)-O(2)	172.4(3)				
C(11)-C(12)-C(17)-C(18)	177.9(3)	C(12)-C(17)-C(18)-C(19)	179.8(2)				
C(13)-C(12)-C(17)-C(8)	179.1(3)	C(17)-C(18)-C(19)-N(1)	177.5(2)				

TABLE-5
HYDROGEN BONDS OF COMPOUNDS I AND II

D-H...A	D-H (Å)	H...A (Å)	D...A (Å)	D-H...A (°)
Compound I				
C(18)-H(18)...O(1)	0.93	2.33	2.918(4)	120.7
C(23)-H(23)...O(2)	0.93	2.37	2.965(5)	121.4
C(29)-H(29)...Cl(1)#1	0.93	2.92	3.548(3)	126.3
Compound II				
C(8)-H(8)...O(2)	0.93	2.33	2.9315(4)	122.2
C(23)-H(23)...O(2)	0.93	2.26	2.886(5)	123.7

Symmetry code: #1 x+1/2, -y+3/2, z+1/2

and d_i, which denotes the distance of any surface point nearest to the interior atoms and the distance of the surface point nearest

to the exterior atoms, respectively and also with the van der Waals (vdW) radii of the atom [56-58]. The red colour circular spots indicate closer hydrogen bonding contacts with negative d_{norm} value. The blue colour indicates longer contacts with positive d_{norm} value and the white colour indicates the intermolecular distances close to van der Waals radii with d_{norm} value equal to zero [59]. The shape index indicates the shape of the electron density surface around the molecular interactions.

Figs. 5 and 6 show the Hirshfeld surface mapped over d_{norm}, shape index, curvature, intermolecular contacts and fragment patches for compounds I and II. The bright red spot shows the C-H...O, C-H...Cl, C-H...π interactions in both the compounds which confirms the XRD results. The red and blue triangle on the shape index and the large flat region on the

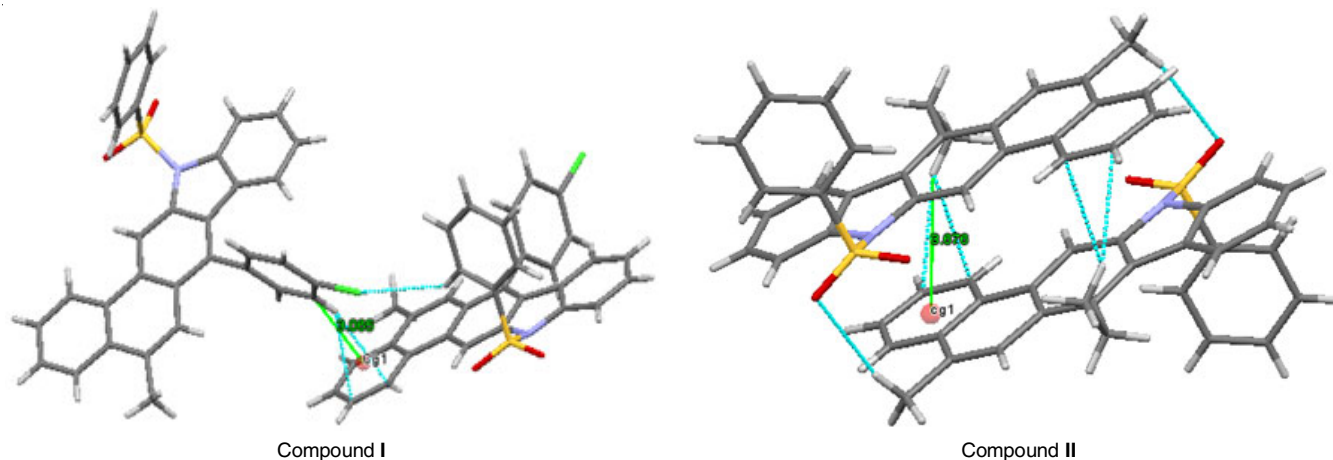


Fig. 4. Crystal packing of compounds **I** and **II** featuring C–H... π interaction

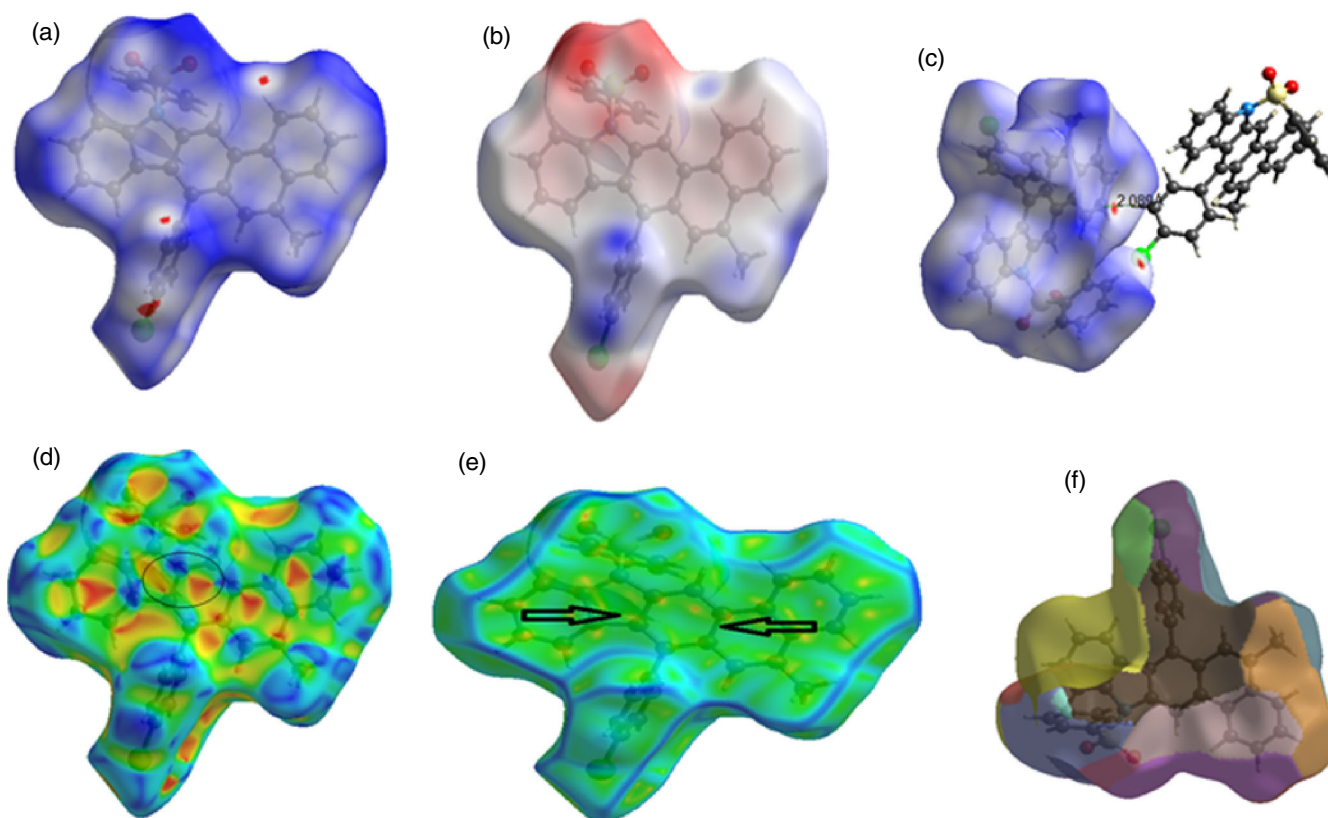


Fig. 5. View of the Hirshfeld surface of compound **I** mapped over (a) d_{norm} and (b) electrostatic potential (c) intermolecular contacts (d) shape index (e) curvature (f) fragment patches

curvature refers to the π ... π interactions. The intermolecular contacts and fragment patches shows the co-ordination environment of the molecule

Figs. 7 and 8 show the percentage of the intermolecular interaction of both compounds. The complete two-dimensional fingerprint plot, are shown in Figs. 7a and 8a and the C...H, C...N, C...C, H...H, H...O and H...Cl interactions are illustrated in Figs. 7a-g and 8a-g. The H...H interactions has the maximum contribution with overall Hirshfeld surface of 41.1 % in compound **I** and 48.3 % in compound **II**. The C...H interactions can be seen as sharp spikes in fingerprint plot showing a contribution of 27.1 % of the Hirshfeld surfaces in compound **I** and 29.7 % in compound **II**. The contribution from the C...N

contacts, can be seen as a shape of bell with a contribution of 1.4 % of the Hirshfeld surfaces in compound **I** and 1.2 % in compound **II**. The C...C contacts, which refers to π ... π stacking interactions, contribute 6.9 % of the Hirshfeld surface in compound **I** and 7.1 % in compound **II**. This appears as a distinct inverted bell shape at around $d_e = d_i \sim 1.7$ Å in both the compounds. The H...O and H...Cl interaction contributes 12.1 and 10.9 % to the total Hirshfeld surfaces in the fingerprint plots in compound **I** and 12.6 % in compound **II**.

The four components electrostatic, polarization, dispersion and exchange repulsion express the interaction energy between the molecules. These energies were obtained using monomer wavefunctions calculated at the B3LYP/6-31G(d,p)

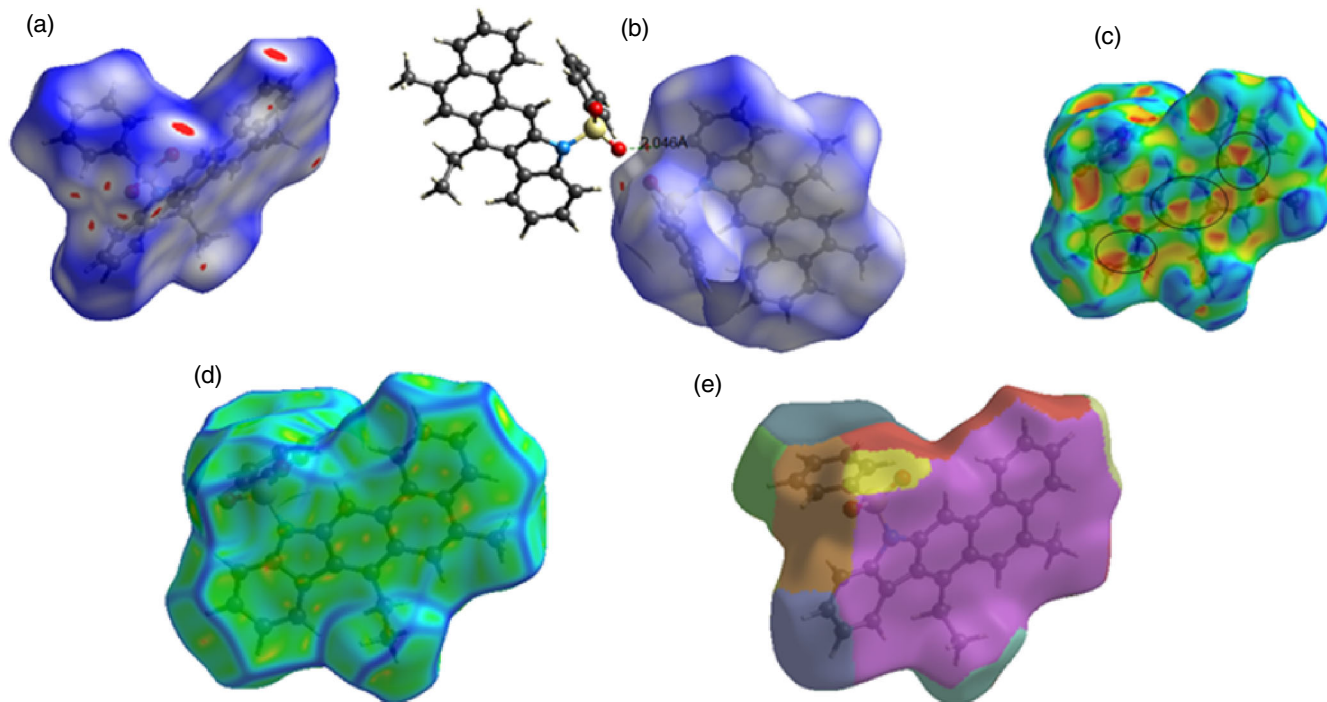


Fig. 6. View of the Hirshfeld surface of compound **II** mapped over (a) d_{norm} and (b) intermolecular contacts (c) shape index (d) curvature (e) fragment patches

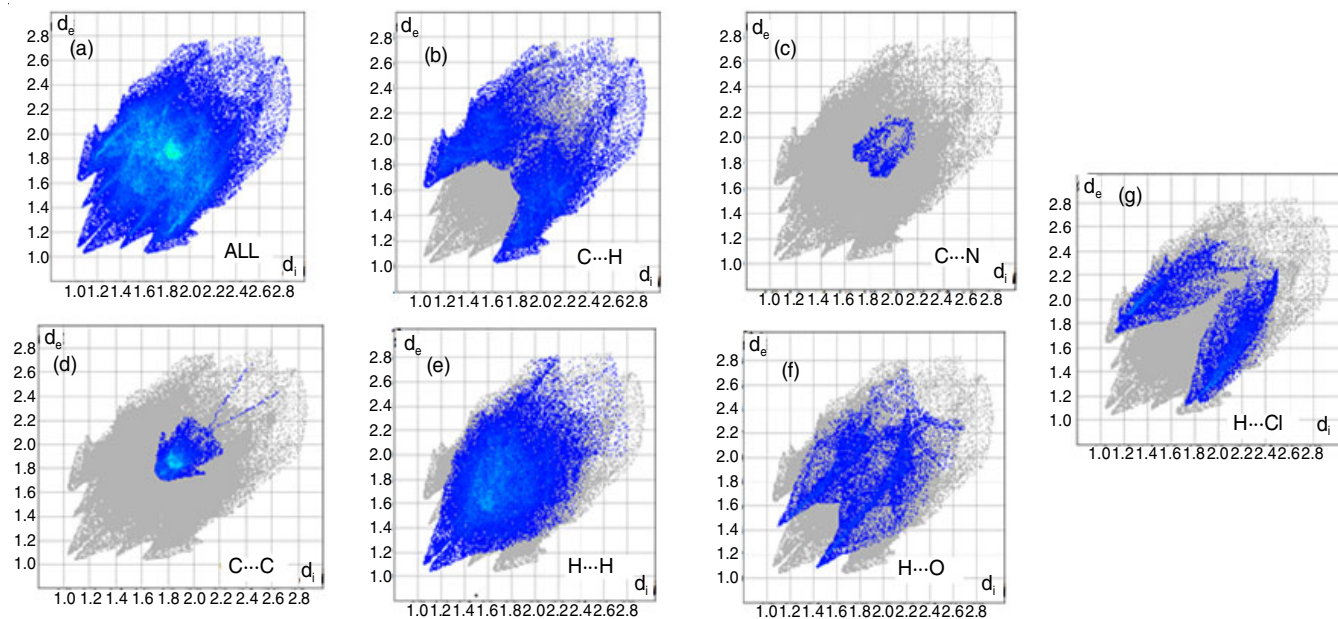


Fig. 7. Two-dimensional fingerprint plots for (a) all interactions, (b) C...H, (c) C...N, (d) C...C, (e) H...H and (f) H...O (g) H...Cl interactions

level. The total interaction energy, which is the sum of scaled components, was calculated for a 3.8 Å radius cluster of molecules around the selected molecule (Figs. 9a and 10a). The interaction energies calculated by the energy model discloses that the interactions in crystal have a important contribution from dispersion components of compounds **I** and **II** (Table-6). The magnitudes of the intermolecular interaction energies are represented graphically using energy frameworks and the supramolecular architecture of the crystal structures are shown in Figs. 9b-9d and 10b-10d.

Molecular docking analysis: Molecular docking aims to attain an optimized conformation for both the protein and

drug with relative orientation between them such that the free energy of the overall system is minimized. Both compounds were developed and the three-dimensional structure was generated using Chem Draw Ultra, 11.0. Ligand molecule was structurally confirmed and energy minimized using Gaussian 03W [60]. The docking studies of both compounds were performed with the selenium-containing target protein, thioredoxin reductase. Three-dimensional structures of target protein thioredoxin reductase (PDB ID: 3QFA) were recovered from the Protein Data Bank (PDB), (<http://www.pdb.org>). The redox protein thioredoxin is involved in numerous cellular processes including activation of ribonucleotide reductase, activation of

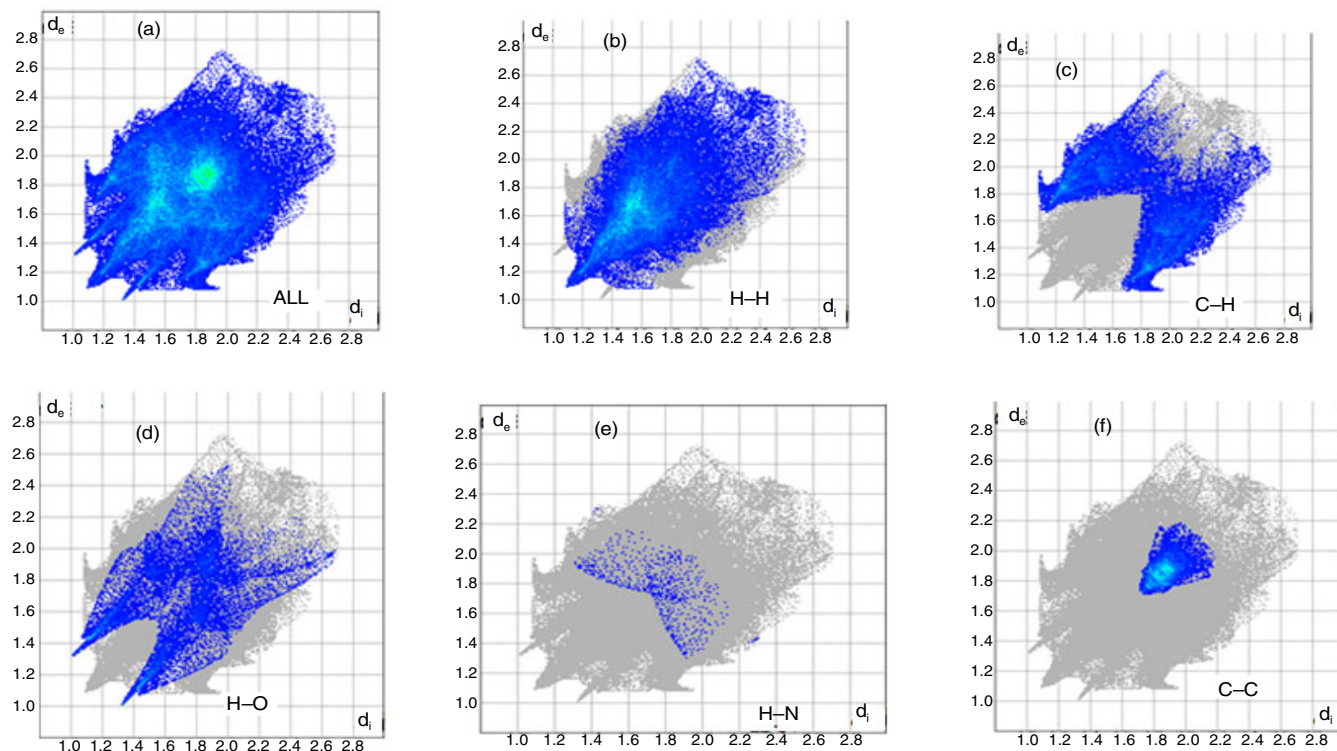


Fig. 8. Two-dimensional fingerprint plots for (a) all interactions, (b) H...H, (c) C...H, (d) H...O, (e) H...N and (f) C...C interactions

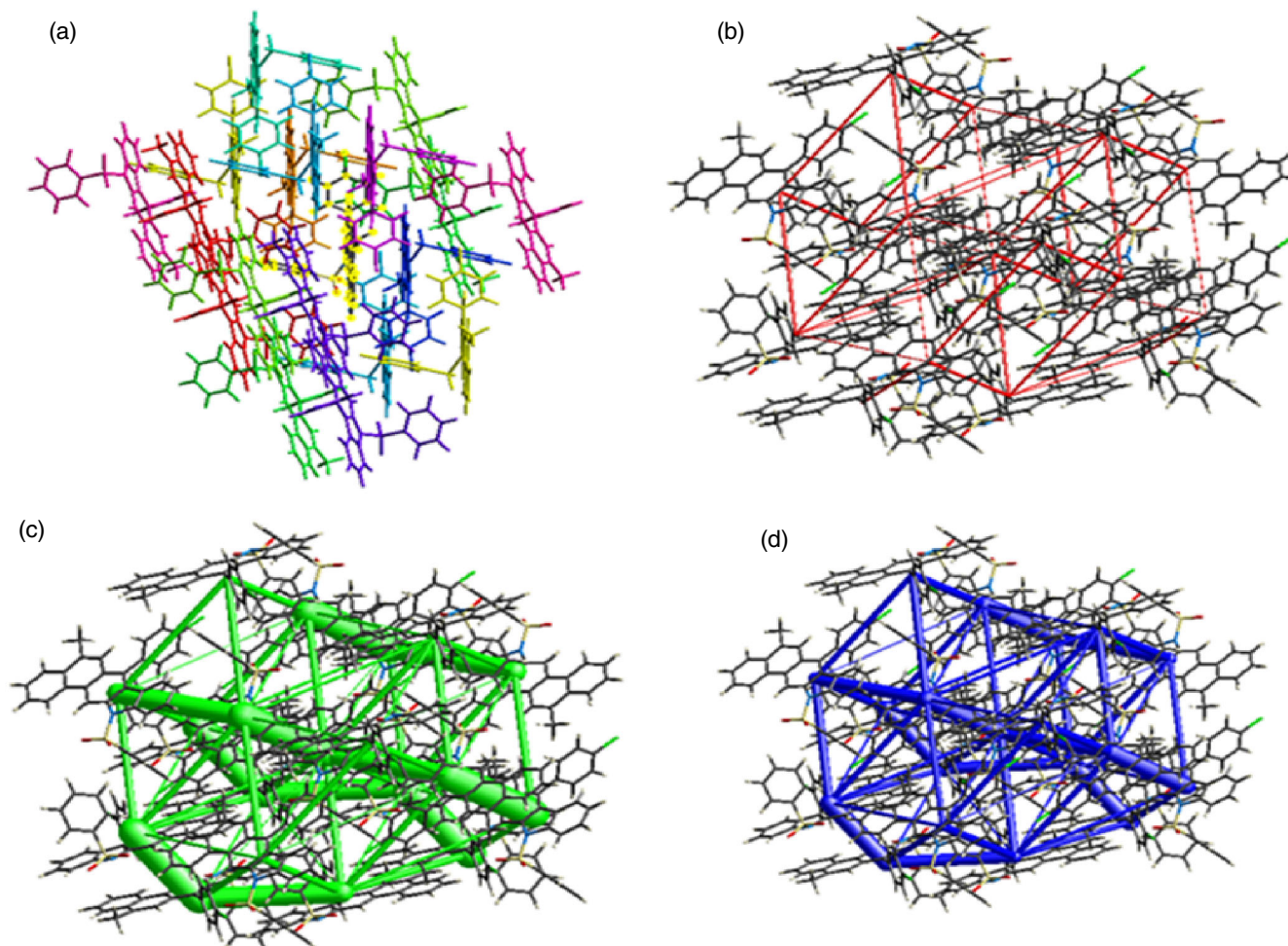


Fig. 9. (a) Interactions between the selected reference molecule (highlighted in yellow) and the molecules present in a 3.8 Å cluster around it, (b) Coulomb energy framework, (c) dispersion energy framework and (d) total energy framework

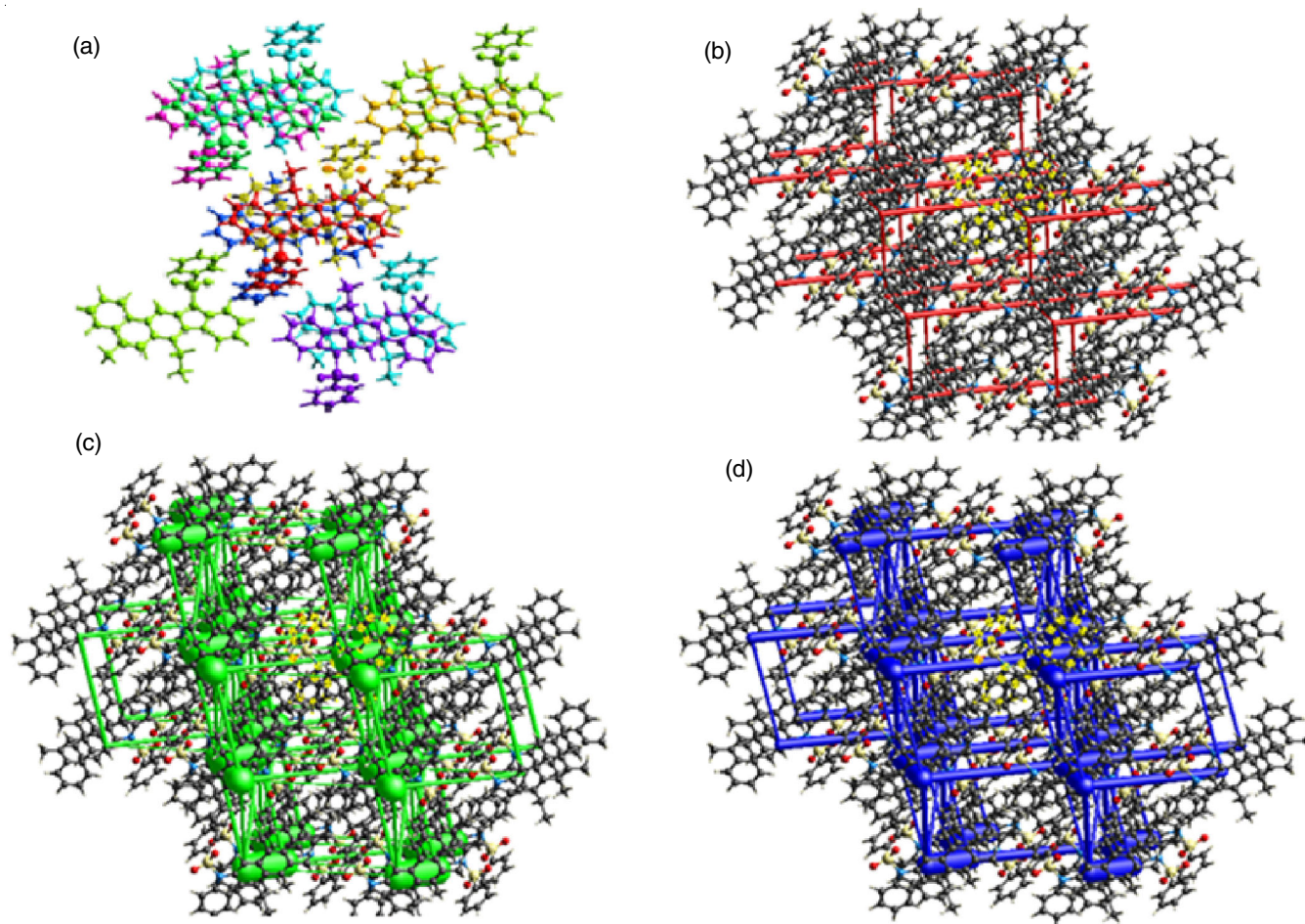


Fig. 10. (a) Interactions between the selected reference molecule (highlighted in yellow) and the molecules present in a 3.8 Å cluster around it, (b) Coulomb energy framework, (c) dispersion energy framework and (d) total energy framework

TABLE-6								
INTERACTION ENERGIES (kJ mol ⁻¹) FOR COMPOUNDS I AND II BETWEEN A REFERENCE MOLECULE AND ITS NEIGHBOURS								
	N	Symp	R	E _{ele}	E _{pol}	E _{dis}	E _{rep}	E _{tot}
Compound I								
	1	-x, -y, -z	7.92	-2.9	-5.7	-98.0	46.3	-57.3
	0	-x+1/2, y+1/2, -z+1/2	9.39	-14.3	-4.9	-33.7	12.6	-38.0
	2	x, y, z	12.86	1.8	-0.3	-4.6	0.1	-2.4
	2	x+1/2, -y+1/2, z+1/2	10.57	-11.4	-2.6	-29.9	17.3	-26.3
	2	x+1/2, -y+1/2, z+1/2	11.97	0.5	-0.7	-5.7	0.1	-5.0
	1	-x, -y, -z	12.94	-3.8	-0.8	-8.7	3.0	-9.8
	2	x, y, z	11.68	-2.7	-3.0	-12.8	3.9	-13.1
	1	-x, -y, -z	5.92	2.7	-12.7	-133.2	57.6	-78.9
	2	-x+1/2, y+1/2, -z+1/2	12.86	-6.1	-2.1	-15.0	3.7	-18.2
	1	-x, -y, -z	11.83	-6.2	-1.6	-34.4	14.3	-26.8
	2	x+1/2, -y+1/2, z+1/2	13.12	0.4	-0.2	-1.7	0.0	-1.2
Compound II								
	1	-x, -y, -z	5.95	-17.1	-7.4	-132.4	61.2	-91.9
	1	-x, -y, -z	10.76	-27.3	-9.5	-23.3	9.9	-47.0
	2	x, y, z	14.22	2.2	-0.9	-8.8	3.1	-3.7
	1	-x, -y, -z	9.71	-4.2	-2.4	-23.3	12.1	-17.0
	2	x, y, z	9.78	1.7	-1.4	-25.9	7.1	-16.7
	1	-x, -y, -z	5.58	-8.9	-12.8	-137.4	65.9	-87.8
	1	-x, -y, -z	12.96	0.7	-0.3	-6.9	3.4	-2.9
	1	-x, -y, -z	9.80	-14.8	-7.3	-19.7	11.7	-28.0

the transcription factor and regulation of photosynthesis [61]. Several lines of evidence suggest human thioredoxin also serves as an extracellular growth factor and plays a role in the promotion of a variety of tumors [62]. The adult T-cell leukemia derived factor (ADF)1 produced by human lymphocytes transformed with human T-lymphotrophic virus type I has been identified as thioredoxin [63] and human primary solid tumors from lung [64] and colon overexpress thioredoxin.

Thioredoxin can stimulate cell growth in several human solid tumor cell lines, both in cell culture and in scid mice [65] suggesting that the growth-promoting activity of thioredoxin is quite general. Mechanically, growth stimulation by thioredoxin is not well understood, but a functional active site dithiol is required for the activity. The final coordinates for the diamide-oxidized and D60N mutant thioredoxin structures have been deposited with the Brookhaven Protein Data Bank (PDB ID: 1AIU). Fig. 11 shows the protein structure of thioredoxin.

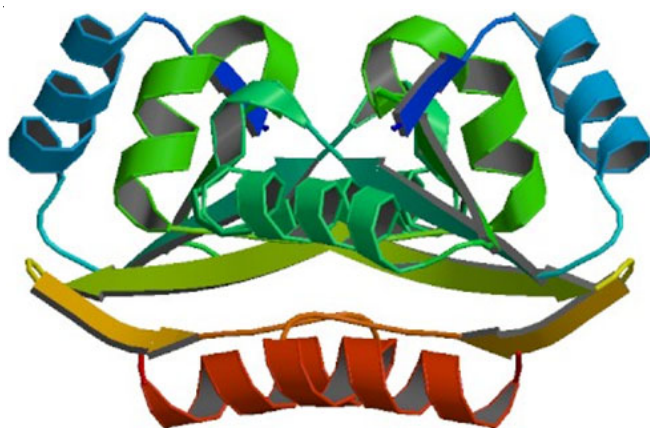


Fig. 11. Protein structure of thioredoxin structure

The active site of the protein was defined to include residues of the active site within the grid size of $92 \text{ \AA} \times 94 \text{ \AA} \times 98 \text{ \AA}$ for compound **I** and $90 \text{ \AA} \times 90 \text{ \AA} \times 90 \text{ \AA}$ for compound **II**.

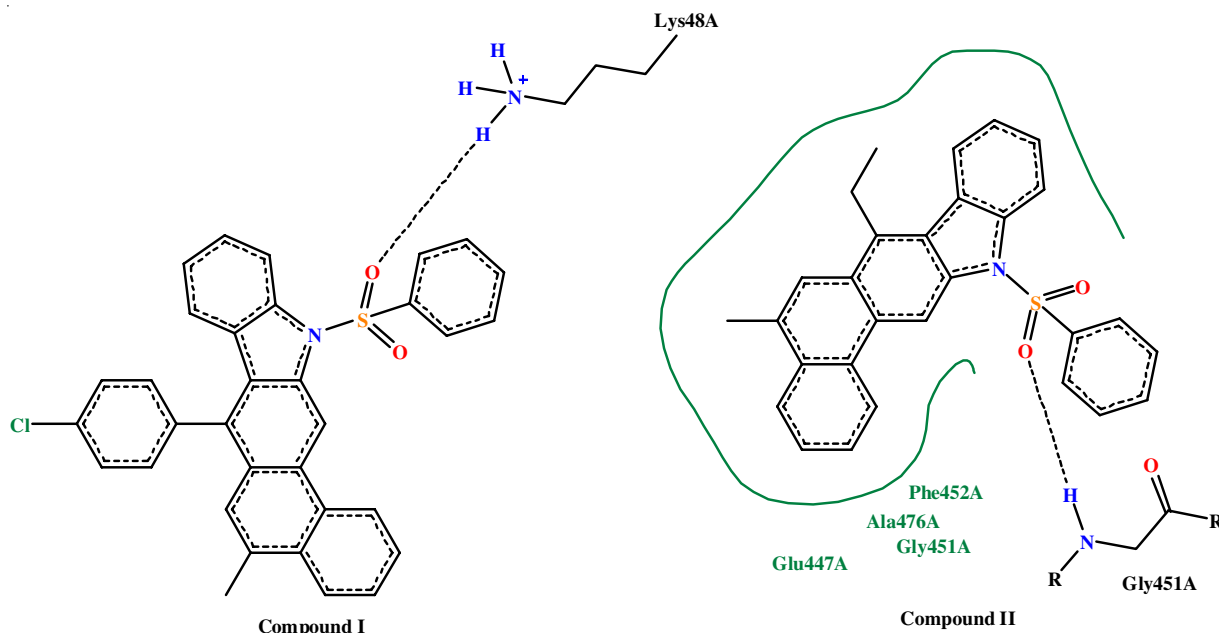


Fig. 12. Poseview diagram of compounds **I** and **II** with 1AIU interactions

The most popular algorithm, Lamarckian Genetic Algorithm (LGA) available in auto dock was employed for docking studies. The docking protocol predicted the same conformation as was present in the crystal structure with RMSD value within the reliable range of 2 \AA for both compounds. Fig. 12 shows the Poseview diagram of compounds **I** and **II** with 1AIU interactions. The docking results give the binding mode of the compounds in the different binding pockets with 1AIU, defined by the amino acid residues. The docking shows that the oxygen atom O1 makes noticeable H bonding interactions with the N-H of Lys48A in compound **I** and in compound **II** S=O with GLY451A. The distance of this hydrogen bonding in compound **I** and **II** are 2.3 and 2.5 \AA , respectively. The interaction found between the protein and the lead in compound **I** and **II** are -7.12 and -5.92 kcal/mol , respectively. These results suggest that the compound exhibits antitumor activity.

Conclusion

Both compounds (**I** and **II**) were synthesized and the structures were confirmed using X-ray diffraction method. In the crystal, molecules are linked by C-H...O and C-H...Cl hydrogen bonds. In the crystals, there are two intramolecular C-H...O hydrogen bonds, which generates two S(6) ring motifs. In both compounds the molecules are linked by C-H...O, C-H...Cl, hydrogen bonds. The molecule also features C-H... π interactions. The Hirshfeld surface analysis confirms the XRD data of intermolecular interactions as bright red spots. The docking protocol predicted the same conformation as was present in the crystal structure with RMSD value within the reliable range of 2 \AA . The docking result shows that the compounds exhibit antitumor activity.

Supplementary data

Crystallographic data for the structural analysis have been deposited with the Cambridge Crystallographic Data Center, CCDC reference numbers: 1569609, 1867913. Copies of this information may be obtained free of the charge from the Director, CCDC, 12 Union Road, Cambridge, CB2 1EZ, UK

(Fax: +44-1223-336033; E-mail: deposit@ccdc.cam.ac.uk or <http://www.ccd.cam.ac.uk>).

ACKNOWLEDGEMENTS

The authors wish to acknowledge the SAIF, IIT Madras, Chennai, India for the data collection.

CONFLICT OF INTEREST

The authors declare that there is no conflict of interests regarding the publication of this article.

REFERENCES

- K. Zhang, Y. Tao, C. Yang, H. You, Y. Zou, J. Qin and D. Ma, *Chem. Mater.*, **20**, 7324 (2008); <https://doi.org/10.1021/cm802240q>.
- P. Rani, V.K. Srivastava and A. Kumar, *Eur. J. Med. Chem.*, **39**, 449 (2004); <https://doi.org/10.1016/j.ejmech.2003.11.002>.
- H. Panwar, R.S. Verma, V.K. Srivastava and A. Kumar, *Indian J. Chem.*, **45B**, 2099 (2006).
- E. Abele, R. Abele, O. Dzenitis and E. Lukevics, *Chem. Heterocycl. Compd.*, **39**, 3 (2003); <https://doi.org/10.1023/A:1023008422464>.
- M. Itoigawa, Y. Kashiwada, C. Ito, H. Furukawa, Y. Tachibana, K.F. Bastow and K.H. Lee, *J. Nat. Prod.*, **63**, 893 (2000); <https://doi.org/10.1021/jf0100020e>.
- R.S. Ramsewak, M.G. Nair, G.M. Strasburg, D.L. DeWitt and J.L. Nitiss, *J. Agric. Food Chem.*, **47**, 444 (1999); <https://doi.org/10.1021/jf9805808>.
- Y. Tachibana, H. Kikuzaki, N.H. Lajis and N. Nakatani, *J. Agric. Food Chem.*, **49**, 5589 (2001); <https://doi.org/10.1021/jf010621r>.
- W. Gu, C. Qiao, S.F. Wang, Y. Hao and T.T. Miao, *Bioorg. Med. Chem. Lett.*, **24**, 328 (2014); <https://doi.org/10.1016/j.bmcl.2013.11.009>.
- S. Thiramatrakul, C. Yenjai, P. Waiwut, O. Vajragupta, P. Reubroycharoen, M. Tohda and C. Boonyarat, *Eur. J. Med. Chem.*, **75**, 21 (2014); <https://doi.org/10.1016/j.ejmech.2014.01.020>.
- F. Giraud, M. Bourhis, L. Nauton, V. Théry, L. Herfindal, S.O. Døskeland, F. Anizon and P. Moreau, *Bioorg. Chem.*, **57**, 108 (2014); <https://doi.org/10.1016/j.bioorg.2014.09.004>.
- C. Asche and M. Demeunynck, *Anticancer Agents Med. Chem.*, **7**, 247 (2007); <https://doi.org/10.2174/187152007780058678>.
- H.J. Knölker and K.R. Reddy, *Chem. Rev.*, **102**, 4303 (2002); <https://doi.org/10.1021/cr020059j>.
- S. Ye, Y. Liu, J. Chen, K. Lu, W. Wu, C. Du, Y. Liu, T. Wu, Z. Shuai and G. Yu, *Adv. Mater.*, **22**, 4167 (2010); <https://doi.org/10.1002/adma.201001392>.
- R.H. Friend, R.W. Gymer, A.B. Holmes, J.H. Burroughes, R.N. Marks, C. Taliani, D.D.C. Bradley, D.A. Dos Santos, J.L. Brédas, M. Löglund and W.R. Salaneck, *Nature*, **397**, 121 (1999); <https://doi.org/10.1038/16393>.
- K. Brunner, A. van Dijken, H. Börner, J.J. Bastiaansen, N.M. Kiggen and B.M. Langeveld, *J. Am. Chem. Soc.*, **126**, 6035 (2004); <https://doi.org/10.1021/ja049883a>.
- S.J. Su, H. Sasabe, T. Takeda and J. Kido, *Chem. Mater.*, **20**, 1691 (2008); <https://doi.org/10.1021/cm703682q>.
- S.C. Bang, Y. Kim, M.Y. Yun and B.Z. Ahn, *Arch. Pharm. Res.*, **27**, 485 (2004); <https://doi.org/10.1007/BF02980120>.
- M.A.J.A. Khan and S.S. Shafi, *Asian J. Chem.*, **15**, 1443 (2003).
- T. Vandana and K.R. Prasad, *Asian J. Chem.*, **15**, 1630 (2003).
- A. Bourderioux, P. Kassis, J.Y. Mérour and S. Routier, *Tetrahedron*, **64**, 11012 (2008); <https://doi.org/10.1016/j.tet.2008.09.101>.
- S. Fathalipour, N. Shahrokhnia, A. Afghan and M.M. Baradarani, *Asian J. Chem.*, **22**, 5808 (2010).
- F.F. Zhang, L.L. Gan and C.H. Zhou, *Bioorg. Med. Chem. Lett.*, **20**, 1881 (2010); <https://doi.org/10.1016/j.bmcl.2010.01.159>.
- A.C. Karmakar, G.K. Kar and J.K. Ray, *J. Chem. Soc., Perkin Trans. 1*, 1997 (1991); <https://doi.org/10.1039/p19910001997>.
- S. Routier, G. Coudert and J.Y. Mérour, *Tetrahedron Lett.*, **42**, 7025 (2001); [https://doi.org/10.1016/S0040-4039\(01\)01308-9](https://doi.org/10.1016/S0040-4039(01)01308-9).
- M. Sacak, *J. Appl. Polym. Sci.*, **74**, 1792 (1999); [https://doi.org/10.1002/\(SICI\)1097-4628\(19991114\)74:7<1792::AID-APP22>3.0.CO;2-M](https://doi.org/10.1002/(SICI)1097-4628(19991114)74:7<1792::AID-APP22>3.0.CO;2-M).
- K.S.V. Santhanam and N.S. Sundaresan, *Indian J. Technol.*, **24**, 417 (1986).
- Q. Zhang, J. Chen, Y. Cheng, L. Wang, D. Ma, X. Jing and F. Wang, *J. Mater. Chem.*, **14**, 895 (2004); <https://doi.org/10.1039/b309630k>.
- M. Saravanabhavan, A.F. Ebenazer, V. Murugesan and M. Sekar, *J. Adv. Phys.*, **6**, 30 (2017); <https://doi.org/10.1166/jap.2017.1286>.
- J.V. Grazulevicius, P. Strohriegel, J. Pielichowski and K. Pielichowski, *Prog. Polym. Sci.*, **28**, 1297 (2003); [https://doi.org/10.1016/S0079-6700\(03\)00036-4](https://doi.org/10.1016/S0079-6700(03)00036-4).
- J.H. Burroughes, D.D.C. Bradley, A.R. Brown, R.N. Marks, K. Mackay, R.H. Friend, P.L. Burns and A.B. Holmes, *Nature*, **347**, 539 (1990); <https://doi.org/10.1038/347539a0>.
- K. Meerholz, B.L. Volodin, Sandalphon, B. Kippelen and N. Peyghambarian, *Nature*, **371**, 497 (1994); <https://doi.org/10.1038/371497a0>.
- Y. Wang, Kirk–Othmer Encyclopedia of Chemical Technology, Wiley: New York, vol. 837, edn. 4, p. 18 (1996).
- G. Wang, S. Qian, J. Xu, W. Wang, X. Liu, X. Lu and F. Li, *Physica B*, **279**, 116 (2000); [https://doi.org/10.1016/S0921-4526\(99\)00684-5](https://doi.org/10.1016/S0921-4526(99)00684-5).
- P.L.T. Boudreault, S. Beaupré and M. Leclerc, *Polym. Chem.*, **1**, 127 (2010); <https://doi.org/10.1039/B9PY00236G>.
- S. Beaupré, P.-L.T. Boudreault and M. Leclerc, *Adv. Mater.*, **22**, E6 (2010); <https://doi.org/10.1002/adma.200903484>.
- J. Li and A.C. Grimsdale, *Chem. Soc. Rev.*, **39**, 2399 (2010); <https://doi.org/10.1039/b915995a>.
- J.-F. Morin and M. Leclerc, *Macromolecules*, **35**, 8413 (2002); <https://doi.org/10.1021/ma020880x>.
- W.E. Moerner and S.M. Silence, *Chem. Rev.*, **94**, 127 (1994); <https://doi.org/10.1021/cr00025a005>.
- Y. Zhang, H. Hokari, T. Wada, Y. Shang, S.M. Marder and H. Sasabe, *Tetrahedron Lett.*, **38**, 8721 (1997); [https://doi.org/10.1016/S0040-4039\(97\)10318-5](https://doi.org/10.1016/S0040-4039(97)10318-5).
- S. Grigalevicius, *Synth. Met.*, **156**, 1 (2006); <https://doi.org/10.1016/j.synthmet.2005.10.004>.
- Z.M. Hudson, Z. Wang, M.G. Helander, Z.H. Lu and S. Wang, *Adv. Mater.*, **24**, 2922 (2012); <https://doi.org/10.1002/adma.201200927>.
- X. Zhang, Y. Wu, S. Ji, H. Guo, P. Song, K. Han, W. Wu, W. Wu, T.D. James and J. Zhao, *J. Org. Chem.*, **75**, 2578 (2010); <https://doi.org/10.1021/jo100119v>.
- L.X. Chen, C.G. Niu, G.M. Zeng, G.H. Huang, G.L. Shen and R.Q. Yu, *Anal. Sci.*, **19**, 295 (2003); <https://doi.org/10.2116/analsci.19.295>.
- D. Curriel, A. Cowley and P.D. Beer, *Chem. Commun.*, 236 (2005); <https://doi.org/10.1039/B412363H>.
- X. Zhang, L. Chi, S. Ji, Y. Wu, P. Song, K. Han, H. Guo, T.D. James and J. Zhao, *J. Am. Chem. Soc.*, **131**, 17452 (2019); <https://doi.org/10.1021/ja9060646>.
- C.F. Mackenzie, P.R. Spackman, D. Jayatilaka and M.A. Spackman, *IUCr J.*, **4**, 575 (2017); <https://doi.org/10.1107/S205225251700848X>.
- G.M. Sheldrick, *Acta Crystallogr.*, **A71**, 3 (2015); <https://doi.org/10.1107/S2053273314026370>.
- A.L. Spek, *Acta Crystallogr. D Biol. Crystallogr.*, **65**, 148 (2009); <https://doi.org/10.1107/S090744490804362X>.

49. C.F. Macrae, P.R. Edgington, P. McCabe, E. Pidcock, G.P. Shields, R. Taylor, M. Towler and J. van de Streek, *J. Appl. Cryst.*, **39**, 453 (2006); <https://doi.org/10.1107/S002188980600731X>.
50. G. Chakkaravarthi, N. Ramesh, A.K. Mohanakrishnan and V. Manivannan, *Acta Crystallogr. Sect. E Struct. Rep. Online*, **63**, o3564 (2007); <https://doi.org/10.1107/S1600536807034800>.
51. Y. Liu, G.W. Gribble and J.P. Jasinski, *Acta Crystallogr. Sect. E Struct. Rep. Online*, **63**, o738 (2007); <https://doi.org/10.1107/S1600536806053694>.
52. A. Bassindale, *Third Dimension in Organic Chemistry* (1984).
53. F.H. Allen, O. Kennard, D.G. Watson, L. Brammer, A.G. Orpen and R. Taylor, *J. Chem. Soc., Perkin Trans. 2*, S1 (1987); <https://doi.org/10.1039/p298700000s1>.
54. M.A. Spackman and D. Jayatilaka, *CrystEngComm*, **11**, 19 (2009); <https://doi.org/10.1039/B818330A>.
55. F.L. Hirshfeld, *Theor. Chim. Acta*, **44**, 129 (1977); <https://doi.org/10.1007/BF00549096>.
56. J. Dalal, N. Sinha, H. Yadav and B. Kumar, *RSC Adv.*, **5**, 57735 (2015); <https://doi.org/10.1039/C5RA10501C>.
57. S.K. Wolff, D.J. Grimwood, J.J. McKinnon, M.J. Turner, D. Jayatilaka and M.A. Spackman, *Crystal explorer* (2012).
58. M. Spackman and J.J. McKinnon, *CrystEngComm*, **4**, 378 (2002); <https://doi.org/10.1039/B203191B>.
59. H. Ghalla, N. Issaoui, F. Bardak and A. Atac, *Comput. Mater. Sci.*, **149**, 291 (2018); <https://doi.org/10.1016/j.commatsci.2018.03.042>.
60. M.J. Frisch, G.W. Trucks, H.B. Schlegel, G.E. Scuseria, M.A. Robb, J.R. Cheeseman, J.A. Montgomery, T. Vreven Jr., K.N. Kudin, J.C. Burant, J.M. Millam, S.S. Iyengar, J. Tomasi, V. Barone, B. Mennucci, M. Cossi, G. Scalmani, N. Rega, G.A. Petersson, H. Nakatsuji, M. Hada, M. Ehara, K. Toyota, R. Fukuda, J. Hasegawa, M. Ishida, T. Nakajima, Y. Honda, O. Kitao, H. Nakai, M. Klene, X. Knox, J.E. Li, H.P. Hratchian, J.B. Cross, V. Bakken, C. Adamo, J. Jaramillo, R. Gomperts, R.E. Stratmann, O. Yazyev, A.J. Austin, R. Cammi, C. Pomelli, J.W. Ochterski, P.Y. Ayala, K. Morokuma, G.A. Voth, P. Salvador, J.J. Dannenberg, V.G. Zakrzewski, S. Dapprich, A.D. Daniels, M.C. Strain, O. Farkas, D.K. Malick, A.D. Rabuck, K. Raghavachari, J.B. Foresman, J.V. Ortiz, Q. Cui, A.G. Baboul, S. Clifford, J. Cioslowski, B.B. Stefanov, G. Liu, A. Liashenko, P. Piskorz, I. Komaromi, R.L. Martin, D.J. Fox, T. Keith, M.A. Al-Laham, C.Y. Peng, A. Nanayakkara, M. Challacombe, P.M.W. Gill, B. Johnson, W. Chen, M.W. Wong, C. Gonzalez and J.A. Pople, Gaussian, Inc. Wallingford, CT (2004).
61. H. Eklund, F.K. Gleason and A. Holmgren, *Proteins*, **11**, 13 (1991); <https://doi.org/10.1002/prot.340110103>.
62. J.D. Borsi, C. Csáki, T. Ferencz and W. Oster, *Anticancer Drugs*, **7(Suppl 3)**, 121 (1996); <https://doi.org/10.1097/00001813-199601000-00016>.
63. S. Fujii, Y. Nanbu, H. Nonogaki, I. Konishi, T. Mori, H. Masutani and J. Yodoi, *Cancer*, **68**, 1583 (1991); [https://doi.org/10.1002/1097-0142\(19911001\)68:7<1583::AID-CNCR2820680720>3.0.CO;2-N](https://doi.org/10.1002/1097-0142(19911001)68:7<1583::AID-CNCR2820680720>3.0.CO;2-N).
64. P.Y. Gasdaska, J.E. Oblong, I.A. Cotgreave and G. Powis, *Gene Struct. Exp.*, **1218**, 292 (1994); [https://doi.org/10.1016/0167-4781\(94\)90180-5](https://doi.org/10.1016/0167-4781(94)90180-5).
65. A. Baker, C.M. Payne, M.M. Briehl and G. Powis, *Cancer Res.*, **57**, 5162 (1997).